American Mineralogist, Volume 88, pages 1703–1708, 2003

Calderonite, a new lead-iron-vanadate of the brackebuschite group

JOSÉ GONZÁLEZ DEL TÁNAGO,[1,*] ÁNGEL LA IGLESIA,[2] JORDI RIUS,[3] AND SOLEDAD FERNÁNDEZ SANTÍN[1]

[1]Departamento de Petrología y Geoquímica, Facultad de Ciencias Geológicas, Universidad Complutense, 28040 Madrid, Spain
[2]Instituto de Geología Económica, C.S.I.C., Facultad de Ciencias Geológicas, Universidad Complutense, 28040 Madrid, Spain
[3]Institut de Ciències de Materials de Barcelona, C.S.I.C., Campus de la UAB, 01893 Bellaterra, Catalunya, Spain

ABSTRACT

Calderonite, ideally $Pb_2Fe^{3+}(VO_4)_2(OH)$, a new member of the brackebuschite group, has been found in the upper oxidation zone of two Pb-Zn hydrothermal deposits located at Santa Marta and Azuaga, Badajoz province, Spain. Brackebuschite and calderonite probably form a complete solid solution, locally with important substitution of Cu and Zn for Fe and Mn. The monoclinic cell parameters derived from powder X-ray diffraction (XRD) data are: a = 7.647(5) Å, b = 6.094(1) Å, c = 8.900(2) Å, β = 112.0(2)° and V = 384.5(4) Å^3, and the six strongest lines, d-spacing (Å),(I),(hkl), are: 4.893(4)(011), 4.166(3)(002), 3.242(10) ($\bar{2}$11), 3.058(3)(020), 2.980(5) ($\bar{1}$03) and 2.746(5)(003). Electron microprobe analyses (EMPA) show a certain degree of compositional variation not only between the Santa Marta and Azuaga samples but also among grains from the same locality. A representative formula of Santa Marta calderonite, determined from EMPA, based on 9 O atoms: is $(Pb_{1.950}Ca_{0.004}Ba_{0.015})_{1.969}(Fe^{3+}_{0.892}Cu_{0.059}Zn_{0.008}Al_{0.015})_{0.974}$ $(V_{1.847}As_{0.008}Si_{0.039}P_{0.057})_{1.951}O_{7.507}(OH)_{1.493}$. Fe^{3+} is principally substituted by Cu^{2+}, and V^{5+} by Si^{4+}. ρ_c = 6.05 g/cm^3. The thermogravimetric analysis yields a weight loss of 1.91%, which corresponds to the 1.493 H needed to maintain the charge balance. Differential thermal analysis shows endothermic effects at 279 and 663 °C due to dehydroxylation.

A single-crystal XRD refinement was carried out on a selected crystal with cationic content determined by EMPA and starting atomic positions from brackebuschite. Final R-value of 5.81% based on 952 reflections with $I > 2\sigma_I$, assuming $P2_1/m$ symmetry, the cell dimensions are a = 7.649 Å, b = 6.101 Å, c = 8.904 Å, β = 112.23°.

Calderonite is red orange to red brown, semitransparent to translucent with vitreous luster and red streak and powder. The fracture is splintery. Optically, it is biaxial positive, with a $2V_X$ = 86° and strong dispersion. In plane-polarized light, it is strongly pleochroic (X = light greenish brown, Y = brown, Z = reddish brown).

INTRODUCTION

The new mineral described here (calderonite) was found during the course of a systematic mineralogical study of the metallic deposits of the ~120 km-long Córdoba-Badajoz Shear Zone (CBSZ) in southwestern Spain. Calderonite was found in sphalerite, pyrite, galena, and minor chalcopyrite hydrothermal deposits in two localities of the CBSZ: Santa Marta and Azuaga. Electron microprobe analyses (EMPA) on this mineral show that it is a Pb-Fe vanadate with no Mn.

Calderonite is named after Professor Salvador Calderón, 1852–1911, in recognition of his important contribution to the mineralogy of Spain. The mineral and the name calderonite have been approved by the I.M.A. Commission on New Minerals and Mineral Names (IMA-CNMMN number 2001-022). The type specimen (number MGM-7748) is kept in the Mineralogical Museum of the Instituto Geológico y Minero de España, Madrid, (Spanish Geological Survey). Cotypes are preserved in the following mineralogical museums: Príncipe Felipe de Borbón, Escuela Técnica Superior de Ingenieros de Minas, Madrid, and Canadian Museum of Nature (number CMNMC 83252).

Calderonite is very similar to brackebuschite, a very rare vanadate, described from the Venus and other mines, Sierra Gorda, Argentina (Rammelsberg 1880; Doering 1883; Foley et al. 1997). Brackebuschite also was reported by Herman et al. (1961) from Lukunga, Zaire, but the identification is questionable because that sample has less than 100 ppm Mn and only 0.5 to 0.1 wt% Fe. It has been also reported in Gabon and in two U.S.A. localities by Anthony et al. (2000) without available data in either of them.

Recently, we have found a new brackebuschite locality in Almería (in southeastern Spain). This locality is situated more than 400 km from the CBSZ and is geologically unrelated.

Occurrences

In the CBSZ, some Pb-Zn hydrothermal deposits contain late-stage V mineralizations in their upper oxidation zones. Apalategui et al. (1985) suggested that those mineralizations could be related to the close proximity of amphibolite bodies.

* E-mail: tanago@geo.ucm.es

The relatively high V content of minerals from Santa Marta amphibolite bodies reinforce this hypothesis: our data indicate that the range of V_2O_5 contents (in wt%) is 0.05 to 0.57 for hornblende, 1.08 to 3.53 for rutile, 0.43 to 0.57 for ilmenite, and 0.12 to 0.17 for almandine. Late-stage tectonic movements in the CBSZ were accompanied by hydrothermal processes. Hydrothermal fluids likely transported V from the amphibolite bodies to the ore oxidation zones where secondary V minerals were formed.

In the Santa Marta and Azuaga deposits, the most common V mineral is vanadinite. Other members of the descloizite-mottramite solid solution are also present in minor amounts and are usually observed overgrowing vanadinite. Calderonite is the latest V mineral in the paragenesis. Its chemical weathering yields a massive product, probably amorphous, enriched in Fe, Mn, and Zn, depleted in Pb, and with a negligible amount of V. The details of the two studied deposits and other calderonite occurrences are given below.

Santa Marta deposit

This deposit is located 2 km NW of Santa Marta village (6° 36' E, 38° 37' 45 N) in Las Colmenitas and Los Llanos mine (Muelas et al. 1977). Normally, vanadinite is the earliest V mineral in the paragenesis, followed by descloizite showing strong compositional differences among grains [the average Cu/(Cu + Zn) ratio is approximately 0.44]. Calderonite postdates descloizite, and it has been found only in some cavities of the gossan zone, where the calderonite crystals locally overgrow darker cores of descloizite. Other common secondary minerals of the oxidation zone, not directly associated with calderonite, are wulfenite, mimetite, cerusite, beudantite, adamite, hemimorphite, and smithsonite. Chalcophanite and native Ag are less abundant. Quartz and Ca-Fe carbonates are ubiquitous.

Santa Marta has been chosen as the type locality for calderonite because here this mineral is more abundant than in Azuaga. Besides, calderonite crystals from Santa Marta are of relatively high quality and Mn free.

Azuaga deposit

This deposit is situated in Azuaga, La Muda site (5° 47' 30 E, 38° 20' 20 N). Here, calderonite only appears in a few fractures cutting across altered gneisses, and it is locally associated with mottramite showing an average Cu/(Cu + Zn) ratio of 0.92. The studied calderonite and ore samples were collected from the dumps at the La Muda mine by one of the authors (J.G.T.) in 1984, because there was no access to the in-situ mineralization. Due to the limited amount and small crystal size of the calderonite material from Azuaga, no complete characterization was possible.

Other world calderonite occurrences

Gurbanova et al. (2001) reported a mineral with a formula similar to calderonite from the Venus mine, Sierra Gorda, Argentina. We also have analyzed small (up to 4–5 μm) scattered crystals from Nepomucene mine, Annaberg, Austria, where they form a thin dark yellow crust. The chemical formula of these crystals, derived from a representative EMPA totaling 98.73 wt%, is $(Pb_{1.96}Ca_{0.02})_{1.98}(Fe^{3+}_{0.97}Cu_{0.01}Zn_{0.12}Al_{0.05})_{1.15}(V_{1.85}As_{0.08}P_{0.01})_{1.94}O_8(OH)$. This composition is very close to that of calderonite and far from ideal heyite (Williams 1973), which was reported from this locality by Auer (1998).

Experimental method

Physical and optical properties

At Santa Marta, calderonite usually occurs in empty cavities as scattered clusters of idiomorphic crystals with maximum lengths of 1 mm. The crystals are prismatic to tabular and show terminal faces. They normally form bundles of parallel, striated crystals, locally flattened parallel to elongation (Fig. 1). Individual crystals up to 250 μm are very uncommon. The crystals are semitransparent to translucent, their color is always deep red orange to red brown, and their luster is vitreous or resinous if slightly altered. At Azuaga, the calderonite crystals are of relatively low quality, small (<50 μm), opaque, and show no luster. Both streak and powder of calderonite are red orange, the fracture is splintery, and the Mohs hardness lies between 3 and 4. Calderonite shows no fluorescence under long- or short-wave ultraviolet light.

The optical angles and orientation were measured with a universal stage using transmitted monochromatic yellow light (λ = 589.3 nm). Calderonite is strongly pleochroic with X = light greenish brown, Y = brown, and Z = reddish brown. It is biaxial positive with a strong dispersion and $2V_x = 86°$.

Differential thermal and thermogravimetric analysis

Differential thermal analysis (DTA) and thermogravimetric analysis (TG) were carried out simultaneously with a Seiko Exstar 6000 instrument, using a static air atmosphere and a heating rate of 10°/min. About 15 mg of crystals were handpicked from the Santa Marta sample, with an estimated purity of >98%. The DTA curve for calderonite (Fig. 2) shows three endothermic effects at 279, 666, and 700 °C. The first and the second ones are ascribed to dehydroxylation reactions, i.e., water removal from OH groups. The third one, an asymmetric effect at 700 °C could be ascribed to one of three phenomena: melting of the sample, solid-solid phase transition, or structural collapse of the anhydrous phase. In our opinion, melting is the most probable process because of the sharp exothermic effect observed in the cooling curve at 629 °C, that could be caused by the solidification of the melt. Moreover, it was also observed that the sample was stuck to the platinum sample-pan at the end of the run.

The TG curve shows three steps at temperature intervals 246–308, 308–625, and 625–676 °C, with weight losses of 0.56, 1.35, and 0.48 wt%, respectively. The first and second ones (1.91 wt%) are ascribed to dehydroxylation reactions, and the third one is probably caused by PbO volatilization. The sum of the first and second experimental weight losses determined for the Santa

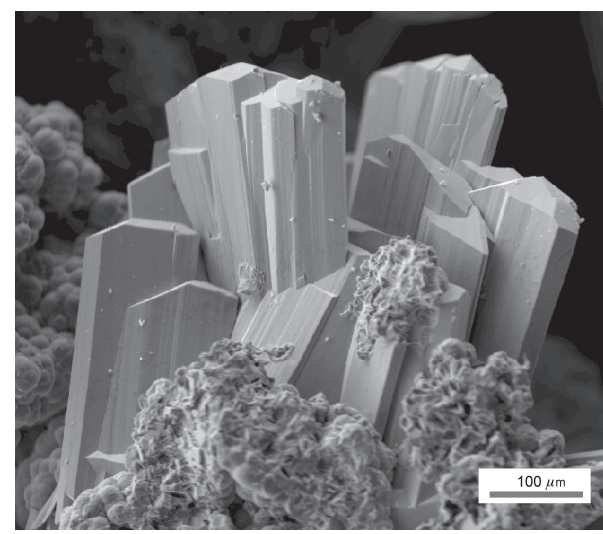

Figure 1. Secondary electron image showing a cluster of prismatic calderonite crystals from Santa Marta, the type locality of calderonite.

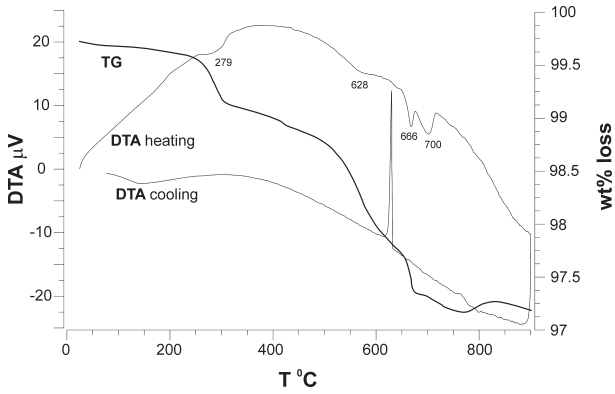

FIGURE 2. DTA and TG curves of calderonite from Santa Marta.

Marta sample and ascribed to water removal (1.91 wt%) agree fairly well with the values reported by Rammelsberg (1880), 2.03 wt%, and by Doering (1883), of 1.92 and 2.43 wt%, for brackebuschite. These are the only three H_2O analyses of this mineral known at present.

Chemical composition

Several crystals and clusters were handpicked from different cavities, mounted in epoxy, and polished. Wavelength-dispersive electron microprobe analyses for calderonite and associated minerals were obtained using a Jeol JXA-8900M instrument at the Universidad Complutense, Madrid. Standard operating conditions were: accelerating voltage 20 kV, probe current 50 nA, peak counting time 10 s and background counting time of 5 s, with a beam diameter of 5 μm. The standards used were galena (Pb*M*α), kaersutite (Mg*K*α, Ca*K*α), benitoite (Ba*L*α), garnet (Mn*K*α, Fe*K*α), chalcopyrite (Cu*K*α), gahnite (Zn*K*α), albite (Na*K*α, Al*K*α), vanadinite (V*K*α, and *K*β were used in the Ti-bearing amphibolite minerals), sillimanite (Si*K*α), fluorapatite (P*K*α), synthetic AsGa (As*L*α), ilmenite (Ti*K*α), and K-feldspar (K*K*α). The results were processed with an on-line ZAF program.

The average composition of the Santa Marta calderonite is given in Table 1. Concentrations of Sn, Bi, Sb, Mo, Ag, Sr, Ge, and Cd were below the detection limit. The chemical composition of calderonite is highly variable among different grains of the same deposit, especially as far as Pb, Cu, Zn, Si, and P are concerned. The large estimated standard deviations (Table 1) are due to the high intergranular compositional variability. Such variability has been also reported for brackebuschite by Foley et al. (1997) and Gurbanova et al. (2001), so that it may be a characteristic of the brackebuschite group. In the case of calderonite, back-scattered electron images locally show a weak zoning caused by small compositional variations within the same crystal. For Santa Marta, the type locality, the average of 21 representative EMPA of different zones and crystals yields, in combination with the H_2O content determined by TG (1.91 wt%.), the following unit formula based on 9 O atoms: $(Pb_{1.950}Ca_{0.004}Ba_{0.015})_{\Sigma 1.968}(Fe^{3+}_{0.892}Cu_{0.059}Zn_{0.008}Al_{0.015})_{\Sigma 0.974}(V_{1.847}Si_{0.039}P_{0.057}As_{0.008})_{\Sigma 1.950}O_{7.507}(OH)_{1.493}$.

Powder X-ray diffraction

The powder XRD pattern of calderonite was measured with a Phillips PW 1730 diffractometer (Bragg-Brentano geometry) with the following experimental conditions: 2θ interval 2–70°; Cu$K\alpha_{1-2}$ radiation; receiving slit 0.1 mm; step size 0.010 (°2θ); time per step 2 s, sample quantity 15 mg. Silicon powder was used as internal standard. The peak positions were calculated with the Phillips PC-APD software. The unit-cell parameters were refined from *d*-values with the UNITCELL program (Holland and Redfern 1997). The indexed powder pattern and refined unit-cell parameters are given in Table 2. The calculated density for calderonite is 6.05 g/cm^3.

Structure refinement

The data were collected with an Enraf Nonious CAD4 four-circle diffractometer and reduced with the suite of programs included in WinGX (Farrugia 1999). Relevant data collection parameters are listed in Table 3.

Since calderonite is isostructural with brackebuschite (Fig. 3), the atomic

TABLE 1. Average EMPA in wt% and unit formula of calderonite crystals from type locality Santa Marta (21 analysis)

PbO	61.80 (1.11)
CaO	0.03 (0.02)
BaO	0.32 (0.24)
Mn_2O_3	<0.01 (0.00)
Fe_2O_3	10.12 (0.52)
CuO	0.67 (0.34)
ZnO	0.09 (0.06)
Al_2O_3	0.11 (0.10)
V_2O_5	23.86 (0.74)
As_2O_5	0.13 (0.47)
P_2O_5	0.57 (0.52)
SiO_2	0.33 (0.27)
H_2O	1.91 –
Total	99.94
Pb	1.950
Ca	0.004
Ba	0.015
Mn	<0.001
Fe^{3+}	0.892
Cu	0.059
Zn	0.008
Al	0.015
V	1.847
As	0.008
P	0.057
Si	0.039
H	1.493

Notes: Standard deviations are given in parentheses. H_2O calculated by TG; unit formula calculated on the basis of 9 O pfu.

TABLE 2. Indexed X-ray powder-diffraction pattern of calderonite of Santa Marta

hkl	I_{obs}	d_{obs} (Å)	d_{cal} (Å)
001	16	8.242	8.251
011	43	4.893	4.902
$\bar{1}11$	12	4.569	4.532
002	34	4.166	4.126
$\bar{2}01$	5	3.874	3.817
111	18	3.641	3.668
$\bar{2}02$	21	3.401	3.389
$\bar{2}11$	100	3.242	3.235
020	25	3.058	3.047
$\bar{1}03$	48	2.980	2.966
021	12	2.857	2.858
003	48	2.746	2.750
211	14	2.601	2.609
$\bar{2}13$	15	2.485	2.486
022	20	2.449	2.451
$\bar{2}21$	5	2.386	2.381
$\bar{3}00$	5	2.356	2.363
$\bar{3}12$	11	2.310	2.307
310	8	2.196	2.203
$\bar{1}23$	9	2.127	2.126
$\bar{3}01$	13	2.078	2.075
$\bar{2}23$	3	2.030	2.030
311	3	1.968	1.964
$\bar{3}04$			1.660
$\bar{4}02$	7	1.900	1.908
$\bar{4}01$			1.881
131	9	1.863	1.866
203			1.861
$\bar{2}31$	10	1.793	1.793
$\bar{1}24$			1.792
$\bar{3}12$	12	1.711	1.711
$\bar{1}15$	8	1.689	1.690
$\bar{3}24$	5	1.646	1.649
$\bar{4}22$	6	1.615	1.617
401			1.613
$\bar{3}22$	4	1.537	1.538
$\bar{1}25$	4	1.524	1.524

Notes: Calculated unit-cell parameters: a = 7.647(5) Å, b = 6.094(1) Å, c = 8.900(2) Å, α = 90°, β = 112.0(2)°, γ = 90°, V = 384.5(4) Å^3.

coordinates of brackebuschite (Foley et al. 1997) were used as starting values for the refinement of calderonite. The refinement was carried out with SHELX-93 (Sheldrick 1993). Initially, the atomic coordinates and the isotropic thermal parameters were refined with V placed at T1 and T2, Fe at M1, and Pb at M1 and M2, using neutral form factors. The second step was the additional refinement of the occupation parameters of T1, T2, M1, M2, and M3. The third and final step was the additional refinement of the anisotropic thermal parameters for all atoms. The final R values are given in Table 3 and the final atomic coordinates, the effective occupancies, and the Ueq coefficients are listed in Table 4. Inspection of Table 4 shows that, as expected, the mean thermal vibration parameter U_{eq} is smaller for the O atoms of the chain (0.018 Å^2) than for the rest (0.032 Å^2). Figure 3 shows a perspective view of the structure with the atom labels. The polyhedral bond distances are listed in Table 5.

The final weighted R-value based on |F|2 with all data is 16.59%. To check the sensitivity of the refinement to the presence of the small cation vacancies, an additional refinement was carried out under identical conditions but with fixed full occupancies for the cation sites. The values of the anisotropic thermal coefficients are in the same order, but the corresponding weighted *R*-value is slightly worse, having increased to 16.81%.

DISCUSSION

Calderonite is isostructural with brackebuschite and consists of discrete fundamental building units formed by chains of edge-sharing M1(O,OH)$_6$ octahedra, <M1-O>: 2.017 Å (6×), placed at the origin of the unit cell and linked to two different types of tetrahedra, T1O$_4$ and T2O$_4$, <T1-O> and <T2-O>: 1.716 Å (4×) and 1.702 (4×), respectively. The two T sites are filled with V but, for T2, both the refined mean bond length and lower scattering power indicate a partial replacement by lighter at-

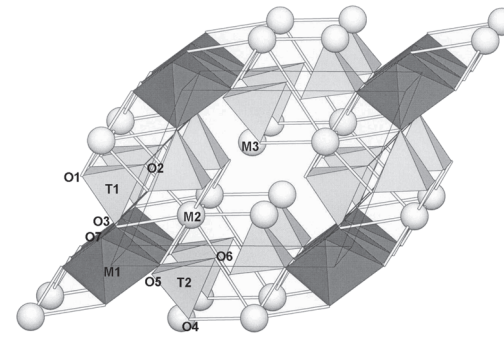

FIGURE 3. Perspective view of the calderonite structure along the **b**-axis (with the **c**-axis across the page) showing the chains of edge-sharing octahedra (Fe^{3+} and Cu^{2+}) and the two different types of symmetry independent vanadate groups (V^{5+}) linked to it. Single-crystal refinement suggests that the cationic sites not belonging to the chains of octahedra are partially empty (≅2.8%). The line going from atom O7 of the chain to atom O2 of one neighboring T1 group represents an H bond. Sites M2 and M3 contain Pb. One of the principal differences with respect to the ideal brackebuschite structure is the probable presence of a proton (≅31% occupancy) bound to O6.

TABLE 3. Crystal data and relevant parameters from structure refinement of calderonite

Dimension	0.27 × 0.07 × 0.07 mm
Unit cell (space group)	$P2_1/m$
a (Å)	7.649(1)
b (Å)	6.101(1)
c (Å)	8.904 (1)
β (°)	112.23(1)
V (Å^3)	384.6
Ideal formula:	$Pb_2 (Fe^{3+}) (VO_4)_2 (OH)$
Z	2
D_{calc} (g/c M^3)	6.04
θ limits (°)	3.0 to 30.37
Number of reflections	1259
Index range	$-10 < h < 10$, $0 < k < 8$, $0 < l < 12$
Number observed reflections	952 with $I > 2\sigma_I$
Variables	85
MoKα radiation	0.71069 Å
μ (cm^{-1})	47.8
T_{min}, T_{max}, T_{av}	0.0448, 0.0810, 0.0068
Absorption correction	Gaussian (106920 sampling points)
*R*1(all data)	0.0775
*wR*2(all data)	0.1659
*R*1 ($I > 2\sigma_I$)	0.0581
Goodness-of-fit (all data)	1.037
$\Delta\rho_{max}$ and $\Delta\rho_{min}$ (e/Å^3)	3.8, –3.0

TABLE 5. Polyhedral bond distances in Å with e.s.d. values in parentheses

T1-O1 (2×)	1.707(11)	T2-O4	1.675(16)
T1-O2	1.649(17)	T2-O5 (2×)	1.727(10)
T1-O3	1.799(12)	T2-O6	1.679(15)
Mean:	1.716	Mean:	1.702
M1-O3 (2×)	2.042(12)	M3-O1 (2×)	2.564(11)
M1-O5 (2×)	1.988(10)	M3-O1' (2×)	2.912(11)
M1-O7 (2×)	2.021(11)	M3-O4	2.884(15)
Mean:	2.017	M3-O4' (2×)	3.144(15)
		M3-O5 (2×)	2.933(10)
M2-O1 (2×)	2.540(11)	M3-O6	2.614(15)
M2-O2	2.739(17)	M3-O7	2.606(11)
M2-O3	3.019(12)	Mean:	2.837
M2-O4	2.607(15)		
M2-O5 (2×)	2.625(10)		
M2-O6	2.826(15)		
Mean:	2.690		

TABLE 4. Refined positional parameters and equivalent isotropic displacement parameters (in Å^2) for calderonite

Site/atom	*x/a*	*y/b*	*z/c*	Mult.	Eff. occu.	U_{eq}
T1 (as V)	0.5587(4)	3/4	0.8250(3)	1/2	0.977 (29)	0.010(1)
T2 (as V)	0.9601(4)	3/4	0.6621(3)	1/2	0.935 (29)	0.009(1)
M1 (as Fe)	0	0	0	1/2	1.015 (28)	0.011(7)
M2 (as Pb)	–0.2614(1)	3/4	0.2554(1)	1/2	0.979 (23)	0.0241(3)
M3 (as Pb)	0.3227(1)	3/4	0.3970(1)	1/2	0.958 (23)	0.0312(3)
O1	0.4922(13)	0.9783(18)	0.7058(13)	1	1	0.023(2)
O2	0.4525(27)	3/4	0.9554(24)	1/2	1	0.040(5)
O3	0.8084(19)	3/4	0.9435(16)	1/2	1	0.018(3)
O4	0.7295(25)	3/4	0.5451(21)	1/2	1	0.035(4)
O5	–0.0107(14)	0.0167(16)	0.2193(11)	1	1	0.020(2)
O6	0.0757(23)	3/4	0.5350(22)	1/2	1	0.029(4)
O7	0.1854(18)	3/4	0.0808(16)	1/2	1	0.015(3)

Notes: E.s.d. values are given in parentheses. U_{eq} is defined as one third of the trace of the orthogonalized U_{ij} tensor.

oms such as Si, As, and/or P. Each apical O atom, O5, of the octahedron is bound to one T2 atom. From the remaining O atoms of the octahedron, O3 is bound to T1, and O7 is an hydroxyl group forming an H bond with atom O2 belonging to the $T1O_4$ tetrahedron of a neighboring building unit (Fig. 3). The building units are held together by the Pb atoms at sites M2 and M3. The geometry of the eightfold-coordinated M2 site is that of a dipyramidal trigonal prism, which is typical for Pb, <M2-O>: 2.690 Å (8×). The environment of site M3 is more irregular with a coordination number of eleven and, as indicated by its lower refined scattering power, Pb in this site is partially replaced by Ba and Ca, <M3-O>: 2.837 Å (11×). Comparison of the individual polyhedral distances of calderonite and brackebuschite (Foley et al. 1997) indicates that the only significant differences are in the octahedra. In brackebuschite, the presence of Mn^{3+} in the octahedra causes distortions due to the Jahn-Teller effect, observed bond lengths: 2.10(2), 1.98(2) and 1.99(2) Å. In calderonite, however, there is no Mn^{3+} and, because all distances are rather similar (respective bond lengths: 2.04(1), 1.99(1) and 2.02(1) Å), no prolate distortions of the polyhedra are found.

To determine the composition of sites T1 + T2, M1, and M2 + M3, the same crystal used for the XRD experiment was analyzed with the electron microprobe (33 sampling points). The following relative atomic compositions were found: V (94.67%), Si (4.36%), As (0.82%), and P (0.15%) for T1 + T2; Fe^{3+} (95.32%), Cu (3.35%), Zn (0.92%), and Al (0.41%) for M1; Pb (98.72), Ba (0.92%), and Ca (0.36%) for M2 + M3. Combination of these data with the refined effective occupancies given in Table 4 leads to the following formula for the studied crystal:

$$(Pb_{1.924}Ba_{0.018}Ca_{0.007})_{\Sigma 1.949}(Fe^{3+}_{0.965}Cu_{0.034}Zn_{0.009}Al_{0.004})_{\Sigma 1.012}$$
$$(V_{1.836}Si_{0.085}As_{0.016}P_{0.003})_{\Sigma 1.940}O_{7.506}(OH)_{1.494}$$

wherein 1.494 H have been introduced to preserve the charge balance. Removal of the 1.494 H content in the form of water represents a weight loss of 1.92%, which agrees well with the experimental weight loss of 1.91% determined by TG. This unit formula is similar to the previous one derived from the average chemical composition and the experimental weight loss.

As already mentioned above, the interpretation of the refinement results strongly suggests that Si, As, and P are predominantly at site T2, and that Ba and Ca partially replace Pb at M3. This result means that sites T1 and M2 are mainly occupied by V and Pb, respectively. This result also allows the cationic distribution in the unit cell to be derived and the balance of bond valences to be calculated easily. The compositions for the various sites are:

T1: $V_{0.977}$	Σ 0.977
T2: $V_{0.859}$, $Si_{0.085}$, $As_{0.016}$, $P_{0.003}$	Σ 0.963
M1: $Fe_{0.965}$, $Cu_{0.03}$, $Zn_{0.009}$, $Al_{0.004}$	Σ 1.012
M2: $Pb_{0.979}$	Σ 0.979
M3: $Pb_{0.945}$, $Ba_{0.018}$, $Ca_{0.007}$	Σ 0.970

The mean occupancy for the sites other than M1 is 0.972(7), and the small dispersion about this value is noteworthy. The balance of valence bond sums for this specific metal distribution is illustrated in Table 6. Inspection of those results demonstrates the plausibility of the refined crystal structure and, in addition, illustrates the distribution of H atoms needed to achieve the formal charge of the O atoms. This situation can be summarized in three points: (1) As already known from brackebuschite, hydroxyl O7-H contributes approximately 0.26 v.u. (valence units) to the bond strength of atom O2 (distance O7···O2 = 2.67 Å). (2) Atom O6 of $T2O_4$ has a charge deficit compensated by 0.31 H. As no close contacts exist to other O atoms, O6-H forms no H bonds [closest contact: O6···O5 = 3.10Å (2×)]. (3) A second H bond (with only 11% occupation) of type O4-H...O1 (distance O4···O1 = 2.78 Å) seems to exist that would be related to the substitution of V^{5+} by of Si^{4+} in the $T2O_4$ groups.

BRACKEBUSCHITE-CALDERONITE: THE Mn^{3+} - Fe^{3+} END-MEMBERS OF A COMPLETE SOLID SOLUTION?

Foley et al. (1997) found two brackebuschite types: one richer in Fe and the other one richer in Mn. They found that

TABLE 6. Balance of bond valences for calderonite calculated according to the logarithmic expression $L(v) = L(1)_{corr} - 2k \log v$, with $L(1)_{cor\,r} = L(1) + 2k \log(\Sigma v_{ideal}/\Sigma v_{real})$, (Allmann 1975)

Atom	½T1	½T2	½ M1	½M2	½ M3	$\Sigma_{C\,V}$	H	$\Sigma_{C\,Vcorr}$
O1	1.707		2.540	2.564, 2.912	2.02		2.02	
	1.24		0.34	0.31, 0.13				
½O2	1.649		2.739		1.67		1.93	
	1.47		0.20			+.26		
½O3	1.799		2.042 (2×)	3.019		1.98		1.98
	0.94		0.47	0.10				
½O4		1.675		2.607	2.884, 3.144(2×)	1.84		1.93
		1.28		0.28	0.14, 0.07		(+.09)	
O5		1.727	1.988	2.625	2.933	2.03		2.03
		1.10	0.54	0.27	0.12			
½O6		1.679		2.826	2.614	1.69		2.00
		1.26		0.16	0.27		(+.31)	
½O7			2.021 (2×)		2.606	1.26		2.00
			0.49		0.28		+.74	
$S_{A\,V}$	4.885	4.730	2.907	1.958	1.946		Σ_H 1.40	
CN	4	4	6	8	11			
2k	0.78	0.78	0.88	0.90	0.90			

Notes: Site compositions: T1 = $V_{0.977}$; T2 = $V_{0.859}$, $Si_{0.085}$, $As_{0.016}$, $P_{0.003}$; M1 = $Fe_{0.965}$, $Cu_{0.034}$, $Zn_{0.009}$, $Al_{0.004}$; M2 = $Pb_{0.979}$; M3 = $Pb_{0.979}$, $Ba_{0.018}$, $Ca_{0.007}$. Upper values = distances in Å; lower values = bond valences. The bond valences due to the H atoms not present in the ideal brackebuschite structure are given in parentheses. Distances O7···O2 = 2.67(2) Å; O1···O4 = 2.78(2) Å; CN = coordination number of the respective polyhedra.

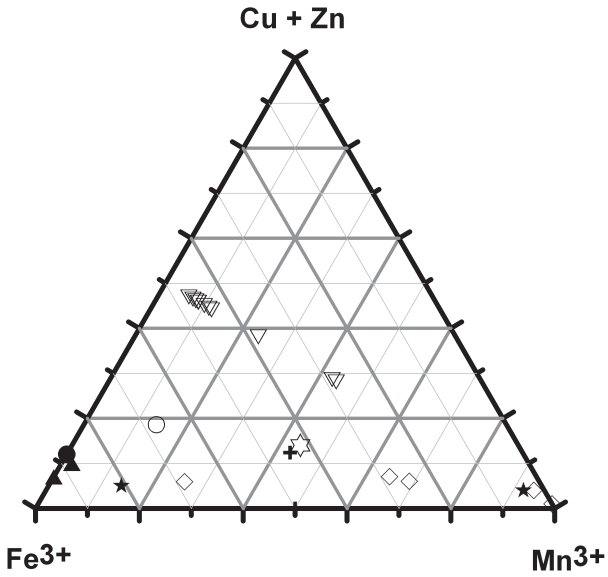

FIGURE 4. Variation of Fe, Mn, Cu-Zn content in known calderonites and brackebuschites. Calderonite: Badajoz, filled-triangles; Annaberg, filled circle. Brackebuschite from Sierra Gorda, Argentina: open star, Rammelsberg (1880); plus signs, Doering (1883); open diamonds, Symes and Williams (1973); filled stars, Foley et al. (1997); open circle, Gurbanova et al. (2001); Brackebuschite from Almería, Spain: open inverted triangles. All analyses have been normalized to one OH group, and with all Fe and Mn as Fe^{3+} and Mn^{3+}.

Mn-rich and Fe-rich regions may coexist even in the same crystal. Due to their similar atomic radii (Mn^{3+} = 0.58 Å and Fe^{3+} = 0.55 Å), the geochemical behavior of Mn^{3+} and Fe^{3+} are very close. A ternary Fe-Mn-(Cu + Zn) plot including all calderonite and brackebuschite compositions known to date is shown in Figure 4. The composition was renormalized by recalculating Mn and Fe as Mn^{3+} and Fe^{3+}, and H_2O, was inferred from by stoichiometry. The Doering (1883) analyses yield: $Pb_{1.90\text{-}1.87}(Mn^{3+}_{0.48–0.57}Fe^{3+}_{0.46–0.51}Cu_{0.04}Zn_{0.11})(V_{1.93–1.96}P_{0.02})O_8(OH)$.

As suggested in Figure 4, brackebuschite and calderonite probably form a solid solution with no compositional gap. These two minerals, along with other Cu-dominated and Zn-dominated members yet to be discovered, might constitute a brackebuschite group of minerals, similar to the descloizite group, which consists of čechite, pyrobelonite, descloizite, and mottramite.

ACKNOWLEDGMENTS

F. Gordillo (1996) found the calderonite mineralization in the Santa Marta mine and provided us with the specimens that were investigated. B. Sainz de Baranda suggested that it could be a new mineral, and supplied the Nepomucene mine specimen. We thank A. Fernández Larios of the Centro de Microscopía Electrónica of the Universidad Complutense for kindly using his analytical experience to obtain best-possible EMPA, and the beautiful SEM images. We thank C. Rosi and J. Abati for their assistance with the English translation and, finally, L.A. Groat and an anonymous reviewer for improving the manuscript. The Spanish MCyT and European FEDER, project no. MAT2002-02808, for financial support (J. Rius).

REFERENCES CITED

Allmann, R. (1975) Beziehungen zwischen Bindungslängen und Bindungsstärken in Oxidstrukturen. Monatshefte für Chemie, 106, 779–793.

Anthony, J.W., Bideaux, R.A., Bladh, K.W., and Nichols, M.C. (2000) Handbook of Mineralogy Vol. IV Arsenates, Phosphates, Vanadates, 680 p. Mineral Data Publishing, Tucson, Arizona.

Apalategui, O., Borrero, J.D., Eguiluz, L., Higueras, P., Roldán, F.J., Quesada, C., and Cueto, L.A. (1985) Memoria del mapa geológico de España a escala 1:50000, hoja 878: Azuaga, 47 p. Instituto Geológico y Minero de España.

Auer, C. (1998) Famous Mineral Localities: The Annaberg District, Lower Austria. Mineralogical Record, 29, 177–198.

Doering, A. (1883) III Brackebuschite, A. Descripción química. Sobre los vanadatos naturales de la provincia de Córdoba, Boletín Academia de Ciencias en Córdoba (República Argentina), 5, 501–505.

Farrugia, L.J. (1999) WinGX Suite for Single Crystal Small Molecule Crystallography. Journal of Applied Crystalography, 32, 837–838.

Foley, J.A., Hughes, J.M., and Lange, D. (1997) The atomic arrangement of brackebuschite, redefined as $Pb_2(Mn^{3+},Fe^{3+})(VO_4)_2(OH)$, and comments on Mn^{3+} octahedral. Canadian Mineralogist, 35, 1027–1033.

Gurbanova, O.A., Rastsvetaeva, R.K., and Chukanov, N.V. (2001) Crystal Structure of a New Representative of the Brackebuschite Group $Pb_2Fe(VO_4)_2(OH)$. Doklady Chemistry, 378, 125–128, translated from Doklady Akademii Nauk, 378, 204–207.

Herman, P., Vanderstappen, R., and Hubaux, A. (1961) Contribution à l´etude des mineraux congolais. Annales Societe Geologique de Belgique, 84, 297–309.

Holland, T.J.B. and Redfern, S.A.T. (1997) Unit cell refinement from powder diffraction data: the use of regression diagnostics. Mineralogical Magazine, 61, 65–77.

Muelas, A., Soubrier, J., García de Figuerola, L., Rivas, P., Hernández Enrile, J.L., and Solar, J.B. (1977) Memoria del mapa geológico de España a escala 1:50000, hoja 828: Barcarrota, 40 p. Instituto Geológico y Minero de España.

Rammelsberg, K.F. (1880) Ueber die Vanadinerze aus dem staat Córdoba in Argentinien. Zeitschrift der Deutschen Geologischen Gesellschaft, 32, 708–713.

Sheldrick, G.M. (1993) A L.S. program for crystal structure refinement. University of Göttingen, Germany.

Symes, R.F. and Williams, S.A. (1973) Heyite and brackebuschite compared. Mineralogical Magazine, 39, 69–73.

Williams, S.A. (1973) Heyite, $Pb_5Fe_2(VO_4)_2O_4$, a new mineral from Nevada. Mineralogical Magazine, 39, 65–68.

MANUSCRIPT RECEIVED AUGUST 15, 2002
MANUSCRIPT ACCEPTED MAY 22, 2003
MANUSCRIPT HANDLED BY ALESSANDRO GUALTIERI